

2014

CFD-Based Correlation Development For Air Side Performance Of Finned And Finless Tube Heat Exchangers With Small Diameter Tubes

Daniel Bacellar

University of Maryland, College Park, United States of America, dfbace@umd.edu

Vikrant Aute

University of Maryland, College Park, United States of America, vikrant@umd.edu

Reinhard Radermacher

University of Maryland, College Park, United States of America, raderm@umd.edu

Follow this and additional works at: <http://docs.lib.purdue.edu/iracc>

Bacellar, Daniel; Aute, Vikrant; and Radermacher, Reinhard, "CFD-Based Correlation Development For Air Side Performance Of Finned And Finless Tube Heat Exchangers With Small Diameter Tubes" (2014). *International Refrigeration and Air Conditioning Conference*. Paper 1410.
<http://docs.lib.purdue.edu/iracc/1410>

This document has been made available through Purdue e-Pubs, a service of the Purdue University Libraries. Please contact epubs@purdue.edu for additional information.

Complete proceedings may be acquired in print and on CD-ROM directly from the Ray W. Herrick Laboratories at <https://engineering.purdue.edu/Herrick/Events/orderlit.html>

CFD-Based Correlation Development for Air Side Performance of Finned and Finless Tube Heat Exchangers with Small Diameter Tubes

Daniel BACELLAR¹, Vikrant AUTE^{2*}, Reinhard RADERMACHER³

^{1,2,3}Center for Environmental Energy Engineering
Department of Mechanical Engineering, University of Maryland
College Park, MD 20742 USA

¹Tel: 301-405-7314, ²Tel: 301-405-8726, ³Tel: 301-405-5286
Email: dfbace@umd.edu, vikrant@umd.edu, raderm@umd.edu

* Corresponding Author

ABSTRACT

Air-to-refrigerant heat exchangers are a key component in air-conditioning and heat pump systems. A great deal of effort is spent on the design and optimization of these heat exchangers. One path towards improving their performance is the transition to smaller hydraulic diameter flow channels. This is evident by the recent introduction of microchannel heat exchangers in the stationary HVAC&R sector. Systematic analyses demonstrates a great potential for improvement in terms of size, weight, refrigerant charge and heat transfer performance by employing small diameter tubes in tube-fin heat exchangers. In particular, tube diameters below 5mm need to be investigated. The in-tube refrigerant flow characteristics are well understood for small diameter tubes and accurate heat transfer and pressure drop correlations are available in the literature. On the air side, however, most of what is available in the literature has none or very limited applicability to small tube diameter tubes. In these situations numerical methods such as CFD are commonly employed in the performance evaluation of tube and fin surfaces. Although CFD is a powerful and reliable tool, it is still computationally expensive if used for evaluating a large number of parameterized geometries. This work presents new CFD-based correlations for finned and finless tube heat exchangers for tube diameter ranging from 2mm to 5mm. The methodology implemented in this work consists of analyzing air-side heat transfer and pressure drop characteristics by using a method called Parallel Parameterized CFD (PPCFD). Maximum Entropy Design (MED) method was used to generate 500 samples to efficiently fill the design space. Multiple non-linear regression is performed to correlate the Colburn j factor and the Darcy friction f factor to the data obtained from the CFD simulations. The new correlations for bare tube heat exchangers reproduce 98.5% of the points within 10% of CFD heat transfer coefficient data and 91.9% of the points for pressure drop. Similarly, for plain fin-and-tube heat exchangers, 82.5% of the points are predicted within 15% for heat transfer coefficient and 93.2% for pressure drop.

1. INTRODUCTION

Significant efforts are being dedicated to design and optimization of compact air-to-refrigerant heat exchangers targeting three main objectives (Webb and Kim, 2005): maximize the heat transfer area per core volume ratio, maximize effectiveness and minimize power consumption, and minimize material consumption (i.e. first costs). Small (< 4mm) hydraulic diameter refrigerant channels have proven to be effective towards meeting these objectives. The air-side performance can benefit from smaller tube diameters and spacing by promoting better mixing and higher velocities increasing heat transfer coefficient to the order of 300W/m².K (Paitoonsurikarn *et al.*, 2000).

Round tube heat exchangers with tube outer diameter greater than 5mm have been widely investigated (Wang *et al.* (2000), Singh *et al.* (2009, 2011), and many other researchers). Performance optimization of these geometries has exhausted their limits. Bare tube heat exchangers had become obsolete since the introduction of efficient extended surfaces to improve overall heat transfer coefficient in small components. However recent studies have shown great potential when moving to diameters below 5mm (Paitoonsurikarn *et al.*, 2000, Saji *et al.*, 2001, Kasagi *et al.*, 2003, Shikazono *et al.*, 2007). Adding fins to such designs should also lead to more promising geometries.

Although great strides have been achieved in the field, it is yet to be fully explored. Not much is known about the physics involved, therefore there are not many correlations to predict the pressure drop and heat transfer coefficient for such geometries. Researchers need to rely on computationally expensive numerical analyses such as CFD and FEM, or exhaustive trial and error experimental testing.

Previous correlations for bare tubes with diameters larger than 9mm have been reported in the literature. Grimison (1937) presented the first correlated experimental data from Hoge (1937) and Pierson (1937) for air-to-refrigerant heat exchangers. Žukauskas (1972) further on extensively investigated friction and heat transfer characteristics of various arrangements for tube bundles using different fluids. With a large number of data Žukauskas (1972) presented, perhaps, the mostly used correlations for bare tube heat exchangers until the date. Some analytical correlations for bare tubes are also available in the literature (Khan *et al.*, 2006). The plain fin-and-tube geometries, on the other hand, have a larger number of correlations available. McQuiston (1978) proposed the first correlations for this application that were later improved by Gray and Webb (1986). The most recent correlations for plate fin-and-tube heat exchangers include those from Wang *et al.* (2000). Their correlation aimed at better accuracy with smaller tube diameters (6.27mm) compared to the previous ones. However none of the above listed correlations are applicable to tube bundles with tube diameters below 5mm.

This work presents CFD-based correlations for bare tube and plain fin-and-tube heat exchangers with less than 5mm tube outer diameters, suitable for current HVAC&R applications. The advantage of using CFD simulations over experimental tests, is that one can explore an unlimited variety of designs and not be constrained by available geometries and test resources. The methodology herein employed uses Maximum Entropy Sampling method (Shewry and Wynn, 1987) to efficiently fill in the design space so that a great amount of strategic information can be retrieved to build the correlations.

It should be noted that developing correlations using CFD simulations can be computationally expensive and takes significant engineering time. Parallel Parameterized CFD (Abdelaziz *et al.*, 2010) is a methodology that automates CFD runs for a given parameterized geometry, thereby significantly reducing the engineering time required to complete the CFD simulations and post-processing.

Lastly, it should be emphasized that there is no substitute for prototype development and testing. But, the development of CFD-based correlations will assist in getting the first prototype close to optimal design thereby resulting in better use of available resources. Furthermore, the CFD-based correlations can later be tuned as more experimental data becomes available. All CFD models were carried out using Gambit® 2.4.6 and ANSYS Fluent® 14.5.

2. HEAT EXCHANGER MODELING AND DATA REDUCTION

The heat exchangers studied are the bare tube and plain fin-and-tube heat exchangers in staggered configuration as shown in Figure 1. The detailed parameter range, also known as the design space, for each geometry is listed in Table 1. The longitudinal and transverse tube pitches are based on the tube outer diameter and are represented as a ratio. The fin thickness value was chosen the same used by Wang *et al.* (2000). A CFD model validation using their data was carried out and we maintained the fin thickness in the further analyses.

Table 1: Heat exchangers design space.

Design Variable	unit	Bare Tubes	Plain fin-and-tube
D_o	mm	2.0 to 5.0	2.0 to 5.0
P_t ratio (D_o)	-	1.5 to 3.0	1.5 to 3.0
P_l ratio (D_o)	-	1.5 to 3.0	1.5 to 3.0
N_r	-	2 to 20	2 to 10
FPI	in^{-1}	N/A	8 to 24
Air face velocity	m/s	0.5 to 7.0	0.5 to 7.0
Fin thickness	mm	N/A	0.115 (fixed)

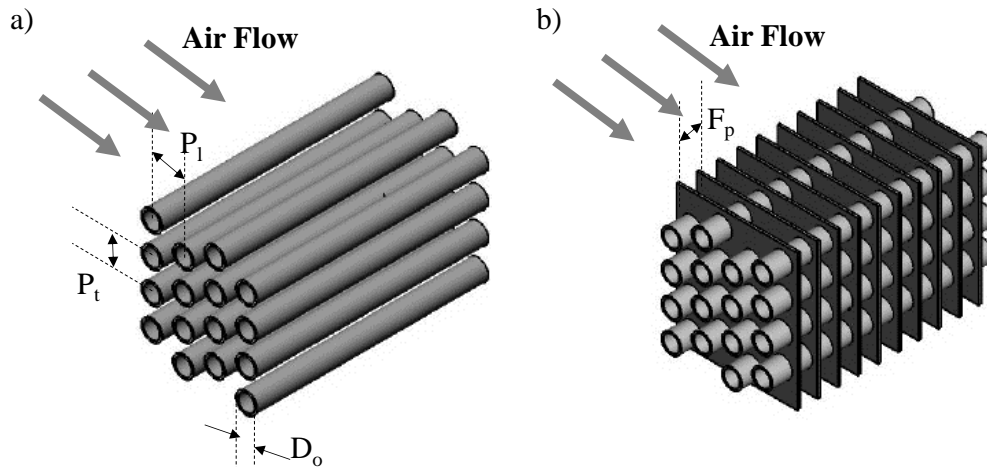


Figure 1: a) Bare Tube Heat Exchanger b) Plain Fin-and-Tube Heat Exchanger.

The heat transfer coefficient can be calculated using the UA-LMTD method (Incropera *et. al.*, 2006) since all temperatures are known from CFD simulations. The CFD models consider only air side whereas the tubes are set to constant wall temperature. The heat rate is calculated based on air mass-weighted average temperatures at inlet and outlet, and it is defined by equation (1).

$$\dot{Q} = \dot{m}_{air} \cdot c_{p_{air}} \cdot (T_{air,out} - T_{air,in}) \quad (1)$$

$$\dot{Q} = UA \cdot LMTD \quad (2)$$

$$LMTD = \frac{(T_w - T_{air,in}) - (T_w - T_{air,out})}{\ln\left(\frac{T_w - T_{air,in}}{T_w - T_{air,out}}\right)} \quad (3)$$

The overall heat transfer coefficient is defined using the same expression used by Wang and Chi (2000), however the tube wall resistance is assumed negligible and the refrigerant side resistance is also negligible since constant wall temperature is assumed.

$$\frac{1}{UA} = \frac{1}{\eta_o h_{air} A_{air}} + \frac{1}{2} \ln\left(\frac{D_o}{D_i}\right) \frac{D_o}{k_w A_w} + \frac{1}{h_{ref} \cdot A_{ref}} \quad (4)$$

Equation (4) can be simplified by the following:

$$h_{air} = \frac{U}{\eta_o} \quad (5)$$

The fin effectiveness is equal to 1 for the bare tubes; for the plain-fin-and-tube an iterative procedure is employed, following a method similar to that described by Wang and Chi (2000). Fin effectiveness and efficiency are defined as per the following equations.

$$\eta_o = 1 - \frac{A_f}{A_o} (1 - \eta) \quad (6)$$

$$\eta = \frac{\tanh(mr\phi)}{mr\phi} \quad (7)$$

$$m = \left(\frac{2h_{air}}{k_f c_f}\right)^{0.5} \quad (8)$$

Where,

$$\phi = (R_{eq} - 1) \left[1 + 0.35 \ln(R_{eq}) \right] \quad (9)$$

$$X_L = \frac{1}{2} \left(\frac{P_t^2}{4} + P_l^2 \right)^{0.5} \quad (10)$$

$$X_M = \frac{P_t}{2} \quad (11)$$

$$R_{eq} = 1.27 \frac{X_M}{r} \left(\frac{X_L}{X_M} - 0.3 \right)^{0.5} \quad (12)$$

The Colburn j factor is determined based on maximum velocity ($u_{\max} = u_{fr}/\sigma$) and is given by the following equation.

$$j = \frac{h_{air}}{\rho_m u_{\max} c_{p_m}} \text{Pr}^{2/3} \quad (13)$$

Air side pressure drop is directly retrieved from air mass-weighted average pressures at inlet and outlet ($\Delta P = P_{in} - P_{out}$). The friction factor is calculated based on the same data reduction in Wang and Chi (2000), with the modification that is also based on maximum velocity.

$$f = \frac{A_{fr}}{A_o} \frac{\rho_m}{\rho_l} \left[\frac{2\Delta P \rho_l}{G_{\max}^2} - (1 + \sigma^2) \left(\frac{\rho_l}{\rho_2} - 1 \right) \right] \quad (14)$$

3. CFD MODELING

The computational domain for bare tube geometry, shown in Figure 2, is a two dimensional cross section of the heat exchanger, longitudinal to air flow direction. End effects are neglected and hence the computational domain is reduced to a single row of tubes. Boundary conditions are defined as constant and homogeneous velocity distribution at inlet, constant pressure at outlet (0.0 Pa gauge), symmetry flow at top and bottom of computational domain, and tubes as walls. The plain fin-and-tube geometry is modeled as a three dimensional computational domain, as shown in Figure 3, with periodic boundaries on the side faces of the computational domain.

A triangular mesh element is set for the two dimensional models, whilst a hexahedron elements are used in the three dimensional models. A refined boundary layer mesh at tube walls is modeled in order to capture the momentum and thermal boundary layers development with higher accuracy.

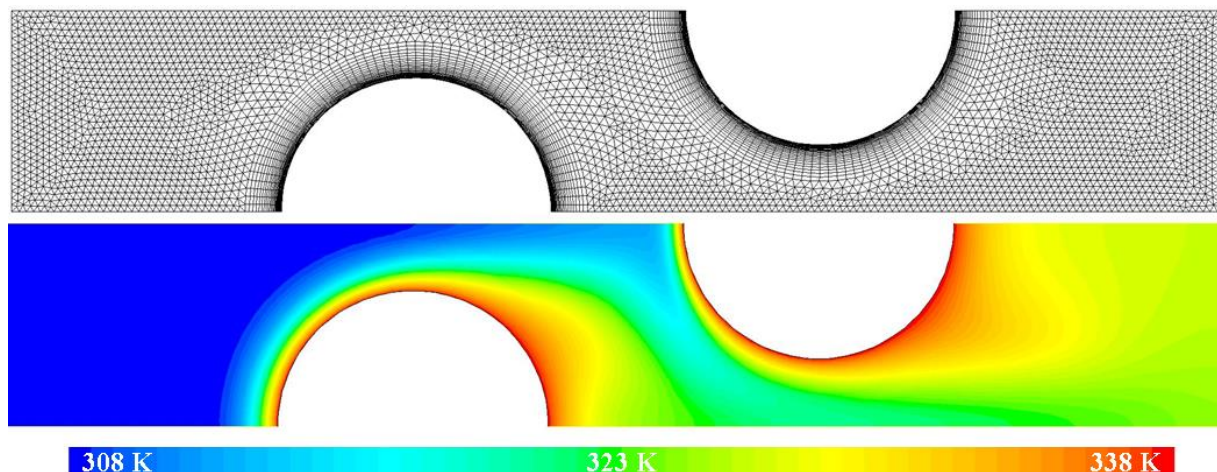


Figure 2: Bare tube computational domain.

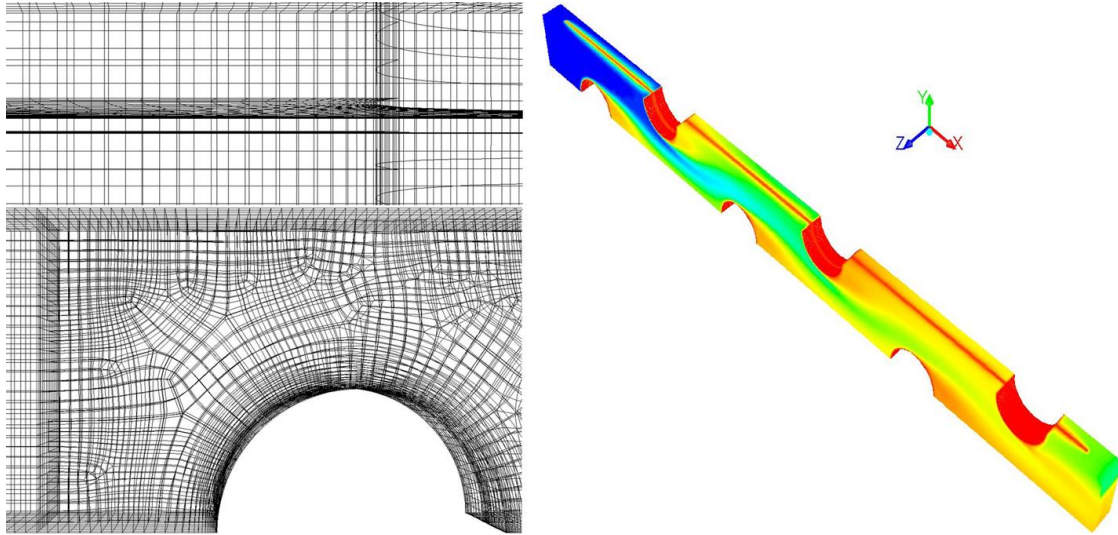


Figure 3: Plain fin-and-tube computational domain.

The air inlet temperature is fixed at 308.15K and is uniform over the face. Tube wall temperature is fixed at 338.15K. The turbulent k- ϵ realizable model is used with enhanced wall functions enabled in every simulation. A second order upwind space discretization is set to ensure better accuracy. Convergence criteria is defined as $1.0e-5$ for continuity and velocities, $1.0e-6$ for energy, and $1e-3$ for turbulent kinetic energy (k) and eddy viscosity (ϵ). Compressibility effects can be neglected since the maximum Mach number, based on maximum velocity is 0.06. Ideal-gas model is used for density, and all the other properties are assumed to be constant.

3.1 Grid Uncertainty Analysis

The Grid Convergence Index (GCI) method, based on Richard Extrapolation (RE) (Roach, 1997, ASME, 2009), is used for Verification and Validation (VV) of the CFD models. Three grids with element size refinement ratio ($r_g = \Delta h_{\text{coarse}} / \Delta h_{\text{fine}}$), of at least 1.3, are investigated for each geometry. The observed order of accuracy (p) is limited between 0.5 and 2.0 to avoid biased uncertainty determination (Oberkampf and Roy, 2007). Since the number of CFD simulations can be very large, the uncertainty analysis is performed for key designs that are expected to exhibit the highest uncertainties. All designs at the boundaries of the design space are then investigated, in addition to the one design at the center of the entire space. The amount of CFD cases to be analyzed is therefore equal to 2^n+1 , where n is the number of design variables. Figure 4 presents the overall uncertainty results for both geometries.

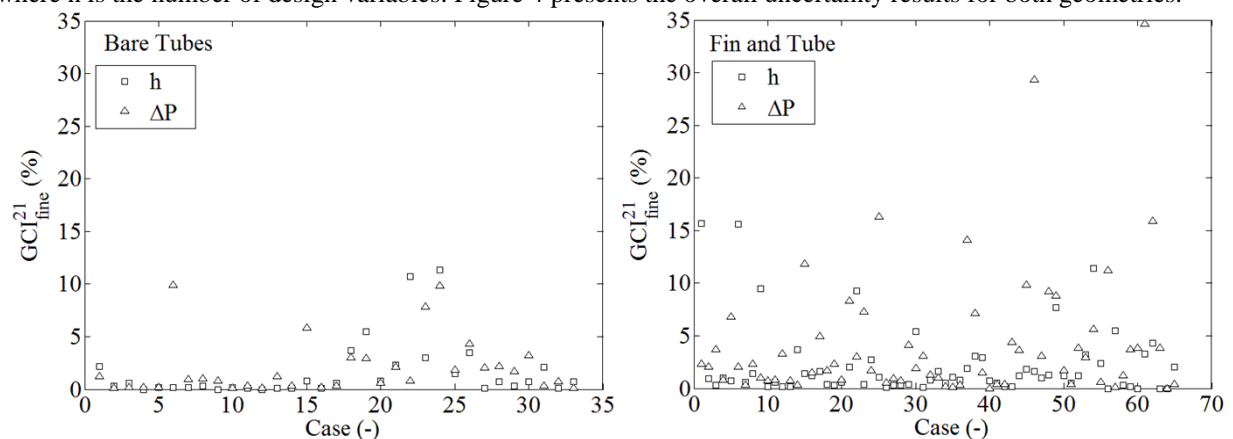


Figure 4: Numerical Uncertainty Analysis.

On average, the bare tube geometries exhibit a mean numerical uncertainty of 1.6% and 2.0% in heat transfer coefficient and pressure drop, respectively. The plain fin-and-tube exhibits an uncertainty of 4.2% and 4.3% in heat transfer coefficient and pressure respectively.

4. CORRELATION DEVELOPMENT

The equation form used for correlation development is based on the one proposed by Wang *et. al.* (2000). Minor modifications were made in order to improve the fit for each correlation. Optimum correlation coefficients are found using MATLAB®'s Goal attainment algorithm to minimize the sum of the errors squared, according to the equations below.

$$\min err_j = \sum_{i=1}^k (j_{CFD,i} - j_{corr,i})^2 \quad (15)$$

$$\min err_f = \sum_{i=1}^k (f_{CFD,i} - f_{corr,i})^2 \quad (16)$$

4.1 Bare Tube Heat Exchanger Correlations

The Colburn j factor is correlated according to equation (17).

$$j = C_1 \text{Re}_{D_o}^{J_1} N_t^{J_2} \left(\frac{P_l}{D_o}\right)^{J_3} \left(\frac{P_t}{D_o}\right)^{J_4} \left(\frac{P_l}{P_t}\right)^{C_2} \quad (17)$$

Where C_i are constants and J_i are defined as follows,

$$J_1 = C_3 + \frac{C_4 N_t}{\ln(\text{Re}_{D_o})} + C_5 \ln \left[N_t \left(\frac{P_l}{D_o}\right)^{C_6} \right] \quad (18)$$

$$J_2 = C_7 + \frac{C_8}{\ln(\text{Re}_{D_o})} \left(\frac{P_t}{D_o}\right)^{C_9} \quad (19)$$

$$J_3 = C_{10} + \frac{C_{11} N_t}{\ln(\text{Re}_{D_o})} \quad (20)$$

$$J_4 = C_{12} + C_{13} \ln \frac{\text{Re}_{D_o}}{N_t} \quad (21)$$

The friction factor is given from the following:

$$f = C_1 \text{Re}_{D_o}^{F_1} N_t^{F_2} \left(\frac{P_l}{D_o}\right)^{F_3} \left(\frac{P_t}{D_o}\right)^{F_4} \left(\frac{P_l}{P_t}\right)^{C_2} \quad (22)$$

Expressions for F_i are identical to those for J_i defined in equations (18) to (21), however different coefficients C_i was found for each.

4.2 Plain Fin-and-Tube

A similar expression is proposed for the plain fin-and-tube correlations.

$$j = C_1 \text{Re}_{D_o}^{J_1} N_t^{J_2} \left(\frac{F_p}{D_c}\right)^{J_3} \left(\frac{P_t}{D_o}\right)^{J_4} \left(\frac{P_l}{D_o}\right)^{C_2} \quad (23)$$

$$J_1 = C_3 + \frac{C_4 N_t}{\ln(\text{Re}_{D_c})} + C_5 \ln \left[N_t \left(\frac{F_p}{D_c}\right)^{C_6} \right] \quad (24)$$

$$J_2 = C_7 + \frac{C_8}{\ln(\text{Re}_{D_c})} \left(\frac{P_t}{D_o}\right)^{C_9} \quad (25)$$

$$J_3 = C_{10} + \frac{C_{11} N_t}{\ln(\text{Re}_{D_c})} \quad (26)$$

$$J_4 = C_{12} + C_{13} \ln \frac{\text{Re}_{D_c}}{N_t} \quad (27)$$

Where,

$$f = C_1 \text{Re}_{D_o}^{F_1} N_t^{F_2} \left(\frac{F_p}{D_c} \right)^{F_3} \left(\frac{F_p}{D_o} \right)^{F_4} \left(\frac{F_p}{P_l} \right)^{C_2} \quad (28)$$

Expressions for F_i are identical to the J_i defined in equations (23) to (27).

5. RESULTS

A total of 500 sample geometries for each heat exchanger type were investigated, with a simulation time ranging from 5 to 15 minutes per sample. With parallel computing, up to 8 simulations were conducted simultaneously. In Figure 5 the dimensionless heat transfer and pressure drop are presented for each population. Table 2 shows the coefficients for each correlation, with precision of the square root of machine's epsilon (10^{-8}). The actual coefficients were calculated with machine's epsilon precision (10^{-16}), however the difference between the numbers presented and the actual ones yield a maximum deviation of the order of 0.000001%. Equations (13) and (14) were used to calculate heat transfer coefficient and pressure drop from the correlations. Figure 6 and Figure 7 show the regression results for bare tubes and fin-and-tube, respectively.

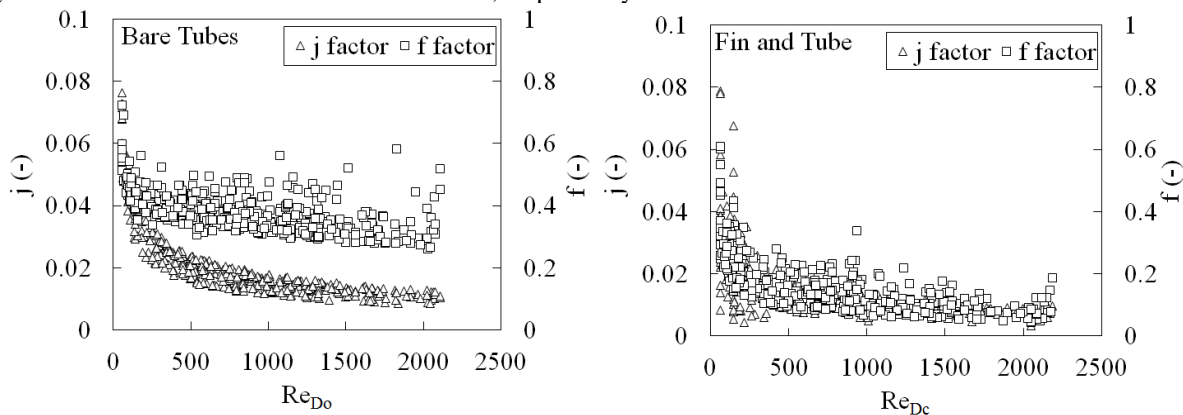


Figure 5: PPCFD results.

Table 2: Correlations coefficients.

Coefficient	Bare Tube		Plain fin-and-tube	
	j	f	j	f
C_1	0.31692086	0.37714526	0.14766977	1.71188871
C_2	0.34727050	0.26992253	-0.28005133	0.92946488
C_3	-0.51134999	-0.04481229	-0.38888827	-0.22854500
C_4	-0.00401654	0.01138922	-0.04370010	0.04029790
C_5	0.09334736	-0.04293416	0.28331915	-0.00430627
C_6	0.52999408	0.77274225	0.44735913	-4.91278551
C_7	-0.97703628	0.21709950	-2.52843969	-0.62616159
C_8	3.10160601	1.73124835	5.29660856	1.31700831
C_9	-0.30758351	-4.97083301	-0.22444323	0.27195519
C_{10}	-0.73451673	-0.18590460	-1.00067472	-2.42919816
C_{11}	0.002349867	-0.01814594	0.30250007	0.06332710
C_{12}	1.34217805	0.56056314	2.08539578	0.97021840
C_{13}	-0.07168253	0.04926124	-0.27444087	0.10375729

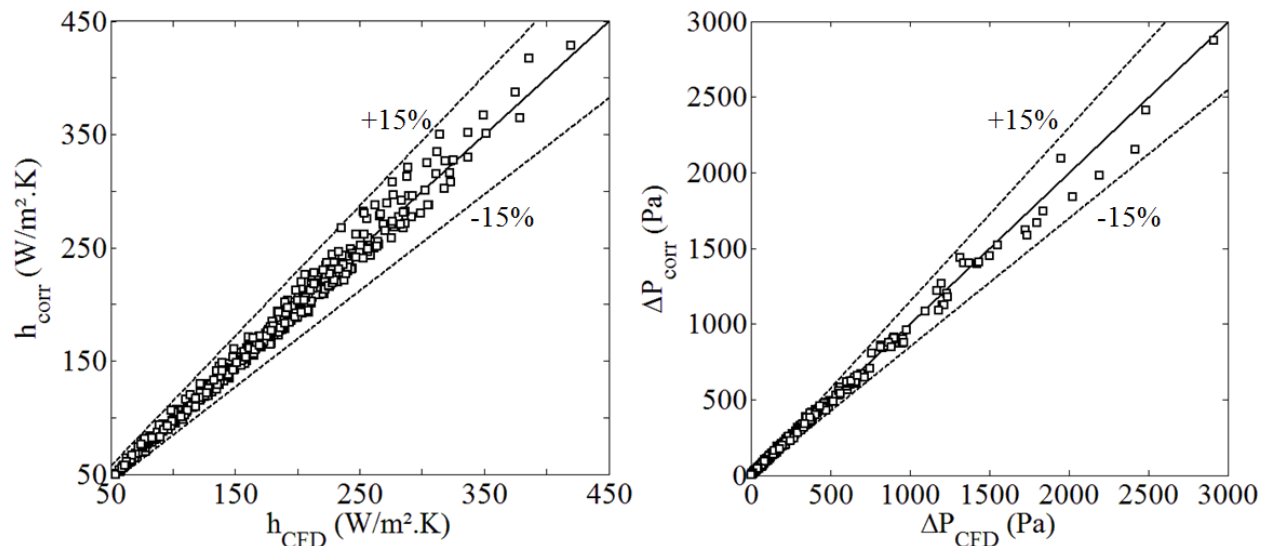


Figure 6: Verification of bare-tube correlation against CFD.

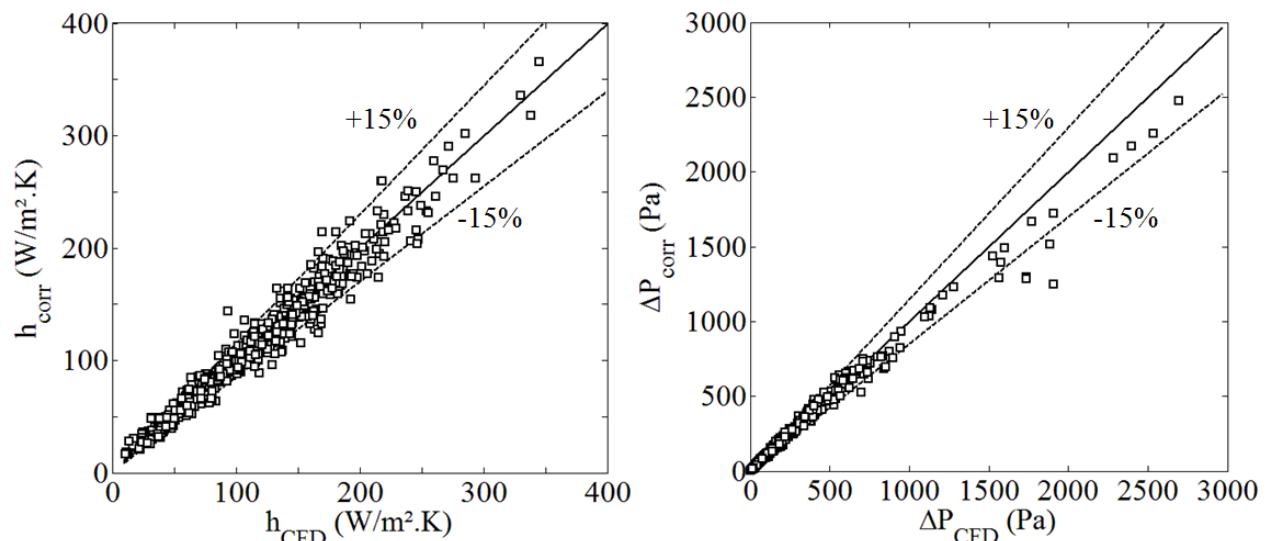


Figure 7: Verification of plain fin-and-tube correlation against CFD.

Table 3: Overall Results.

Heat Exchanger	Bare Tubes		Fin and Tube	
	h_{air}	ΔP_{air}	h_{air}	ΔP_{air}
Air side performance metrics				
10% absolute deviation	98.50%	91.90%	63.58%	79.52%
15% absolute deviation	100.00%	97.90%	82.49%	93.17%
20% absolute deviation	100.00%	99.40%	91.55%	95.98%
30% absolute deviation	100.00%	100.00%	96.98%	98.39%
Absolute relative mean deviation	3.60%	4.40%	9.51%	6.40%
Mean GCI ²¹	1.60%	2.00%	4.20%	4.30%
Coefficient of determination (R^2)	99.60%	98.70%	95.67%	98.53%

6. CONCLUSIONS

This study presents the development of CFD-based correlations for air-side pressure drop and heat transfer coefficients for bare tube and plain fin-and-tube heat exchangers for tube diameters ranging from 2mm to 5mm. CFD simulations were carried out for different geometries and air velocities resulting in a total of 1392 cases. By using the PPCFD method and parallel computing the total time required for simulation was approximately two weeks. Numerical uncertainty quantification was also carried out, and low uncertainties were ensured, especially for bare tubes where excellent agreement between the correlation and CFD results was found. For bare tube case, the proposed correlation predicts more than 90% of the data points within 10%. For the plain fin-and-tube case, more than 80% agree within +/- 15%. Future work includes building prototypes and measuring actual performance for few sample geometries and updating the proposed correlations if necessary. Although experimental validation has not been done yet, these correlations can be used instead of using CFD for design and optimization of air-to-refrigerant heat exchangers thereby saving considerable computational effort. Furthermore, these correlations can also help in choosing the best geometries for prototyping and laboratory testing, thus helping in making the best use of computational and engineering resources.

NOMENCLATURE

A	area	(m ²)
c	specific heat	(J/kg.K)
c _p	specific heat	(J/kg.K)
D _c	collar diameter	(mm)
D _i	inner diameter	(mm)
D _o	outer diameter	(mm)
f	friction factor	(-)
G	mass flux	(kg/m ² .s)
h	heat transfer coefficient	(W/m ² .K)
h	mesh element size	(mm)
j	colburn factor	(-)
k	thermal conductivity	(W/m.K)
\dot{m}	mass flow rate	(kg/s)
N _r	number of tube banks	(-)
P	pressure	(Pa)
P _l	longitudinal tube pitch	(mm)
Pr	Prandtl number	(-)
P _t	transversal tube pitch	(mm)
Q	heat rate	(W)
r	tube outer radius	(mm)
Re	Reynold's number	(-)
R _{eq}	equivalent radius for circular fin	(mm)
r _g	mesh element size ratio	(-)
T	temperature	(K)
u	velocity	(m/s)
UA	global heat transfer coefficient	(W/K)
X _L	center distance between tube banks	(mm)
X _M	half of transversal tube pitch	(mm)

Greek letters

η	fin efficiency	(-)
η_o	fin effectiveness	(-)
ρ	density	(kg/m ³)
σ	contraction ratio	(-)
ϕ	fin efficiency geometrical parameter	(-)

Subscripts

f	fin
fr	frontal
m	mean
ref	refrigerant
w	wall

REFERENCES

- Abdelaziz, O., Aute, V., Azarm, S., Radermacher, R., 2010, Approximation-Assisted Optimization for Novel Compact Heat Exchanger Designs, HVAC&R Research, 16:5, pp. 707-728.
- ANSYS® Academic Research, Release 14.5, 2012, ANSYS Fluent User's Guide, ANSYS, Inc.
- ASME, 2009, Standard for Verification and Validation in Computational Fluid Dynamics and Heat Transfer – Section 2: Code verification, ASME V&V 20 Standard, pp. 7-17.
- Gray, D.L., Webb, R.L., 1986, Heat transfer and friction correlations for plate finned-tube heat exchangers having plain fins, Proc. 8th. Heat Transfer Conference, pp. 2745-2750.
- Grimison, E.D., 1937, Correlation and utilization of new data on flow resistance and heat transfer for cross flow of gases over tube banks, Transactions ASME, 59, pp. 583–594.
- Huge, E.C., 1937, Experimental investigation of effects of equipment size on convection heat transfer and flow resistance in cross flow of gases over tube banks, Transactions ASME 59, pp. 573–581.
- Incropera, F.P., Dewitt, D.P., Bergman, T.L., Lavine, A.S, Fundamentals of heat and mass transfer, John Wiley & Sons.
- Kasagi, N., Suzuki, Y., Shikazono, N., Oku, T., 2003, Optimal design and assessment of high performance micro bare-tube heat exchangers, Proceedings of 4th International Conference on Compact Heat Exchangers and Enhancement Technologies for the Process Industries, pp. 241-246.
- Khan, W.A., Culham, J.R., Yovanovich, M.M., 2006, Convection heat transfer from tube banks in cross flow: Analytical approach, International Journal of Heat and Mass Transfer, 49, pp. 4831-4838.
- MATLAB® and Optimization Toolbox Release 2013a, The MathWorks, Inc., Natick, Massachusetts, United States.
- McQuiston, F.C., 1978, Correlation of heat, mass and momentum transport coefficients for plate-fin-tube heat transfer surface, ASHRAE Transactions, 84(1), pp. 294-308.
- Oberkampf, W. L., and Roy, C. J., 2010, Verification and Validation in Scientific Computing, New York: Cambridge University Press.
- Paitoonsurikarn, S., Kasagi, N., Suzuki, Y., 2000, Optimal design of micro bare-tube heat exchanger, Proceedings of the Symposium on Energy Engineering (SEE2000), vol. 3, pp. 972-979.
- Pierson, O.L. , 1937, Experimental investigation of the influence of tube arrangement on convection heat transfer and flow resistance in cross flow of gases over tube banks, Transactions ASME, 59, pp. 563–572.
- Roache, P. J., 1997, Quantification of uncertainty in computational fluid dynamics, Annu. Rev. Fluid. Mech, 29, pp. 123-160.
- Saji, N., S. Nagai, K. Tsuchiya, H. Asakura, and M. Obata, 2001, Development of a compact laminar flow heat exchanger with stainless steel micro-tubes, Physica, C 354, pp. 148–51.
- Shewry, M.C., Wynn , H.P., 1987, Maximum entropy sampling, Journal of App. Statistics, 14, pp. 165-170.
- Shikazono, N., Okawa, D., Kobayashi, M., Kasagi, N., Waki, T., Kandori, I., Hataya, S., 2007, Research and development of high-performance compact finless heat exchangers, Proceedings of 6th International Conference on Enhanced, Compact and Ultra-Compact Heat Exchangers: Science, Engineering and Technology.
- Singh, V., Aute, V., Radermacher, R., 2009, A heat exchanger model for air-to-refrigerant fin-and-tube heat exchanger with arbitrary fin sheet, International Journal of Refrigeration, 32, pp. 1724-1735.
- Singh, V., Abdelaziz, O., Aute, V., Radermacher, R., 2011, Simulation of air-to-refrigerant fin-and-tube heat exchanger with CFD-based air propagation, International Journal of Refrigeration, 34, pp. 1883-1897.
- Wang, C., Chi, K., 2000, Heat transfer and friction characteristics of plain fin-and-tube heat exchangers, part I: New experimental data, International Journal of Heat and Mass Transfer, 43, pp. 2681-2691.
- Wang, C., Chi, K., Chang, C., 2000, Heat transfer and friction characteristics of plain fin-and-tube heat exchangers, part II: Correlation, International Journal of Heat and Mass Transfer, 43, pp. 2693-2700.
- Webb, R.L., Kim, N., 2005, Principles of Enhanced Heat Transfer, New York: Taylor & Francis, Ch. 2, pp. 1-32.
- Žukauskas, A., 1972, Heat Transfer from Tubes in Cross Flow, in JP Hartnett and TF Irvine Jr., Eds. Advances in Heat Transfer, 8, pp. 93-160.

ACKNOWLEDGMENT

This work was supported by the United States Department of Energy Grant Number DE-EE0006114 and the Integrated Systems Optimization Consortium at the University of Maryland.